

Simulation Study on Different Logic Families of NOT Gate Transistor Level Circuits Implemented Using Nano-MOSFETs

Ooi Chek Yee¹, Lim Soo King²

¹Faculty of Information and Communication Technology, Universiti Tunku Abdul Rahman, Jalan Universiti, Bandar Barat, 31900 Kampar, Perak, Malaysia.

²Lee Kong Chian Faculty of Engineering and Science, Universiti Tunku Abdul Rahman, Jalan Sungai Long, Bandar Sungai Long, Cheras, 43000 Kajang, Selangor, Malaysia.
ooicy@utar.edu.my

Abstract—In this paper, a simulation study has been done on logic NOT transistor circuits with four different logic families, namely: (i) nano-CMOS NOT gate, (ii) nano-MOSFET loaded n-type nano-MOSFET NOT gate, (iii) resistive loaded nano-MOSFET NOT gate, and (iv) pseudo nano-MOSFET NOT gate. The simulation tool used is WinSpice. All the n-type and p-type nano-MOSFETs have channel length (L) 10 nm with width (W) 125 nm or 250 nm, depending on the type of logic families. Simulated timing diagrams for input and output waveforms showed correct logical NOT gate operations for all four logic families. Additionally, the voltage transfer characteristic (VTC) curves have been plotted for all four logic families. From the VTC plots, logic swing (V_{LS}), transition width (V_{TW}), high noise margin (V_{NMH}), low noise margin (V_{NML}), high noise sensitivity (V_{NSH}), low noise sensitivity (V_{NSL}), high noise immunity (V_{NIH}) and low noise immunity (V_{NIL}) have been obtained. Analysis on these values indicated that all the four logic NOT gate families which consist of nano-transistors meet the NOT gate operation conditions. Drain current, intrinsic delay and dynamic power are discussed as the effects of down scaling. In conclusion, NOT gates made of nano-MOSFETs with nanometer dimensions are able to perform correct logical operations in the same way as NOT gates made up of conventional bulk MOSFETs as proven by timing diagrams and VTC plots.

Index Terms—Logic Family; Nano-MOSFET; NOT Gate; Simulation.

I. INTRODUCTION

Downscaling of MOSFET structural dimensions from micrometer regime to nanometer regime has occurred over the last few decades [1, 2, 3]. The conventional bulk CMOS technology is rapidly continuously downscaling until it approaches the scaling limits. The MOSFET channel length L is approaching 10 nm. In order to enable gate to control charge in the channel, the requirement $T_{OX} \ll L$ must be met, where T_{OX} is the oxide thickness [4]. In this study, the gate oxide thickness is approaching 1.5 nm, which is a few atomic layers. Meanwhile, the nano-MOSFET width W used in this study is 125 nm or 250 nm depending on the type of logic families [5, 6, 7]. In this study, NOT logical functions are implemented using four different logic families, namely: (i) nano-CMOS NOT gate, (ii) nano-MOSFET loaded n-type nano-MOSFET

NOT gate, (iii) resistive loaded (800 Ω) nano-MOSFET NOT gate, and (iv) pseudo nano-MOSFET NOT gate. Timing requirements for these NOT gates are analyzed using WinSpice [8, 9, 10]. In addition, VTC curves are plotted using WinSpice and investigations on these VTC curves have shown that all these four NOT gates met the NOT logical operations [11, 12].

II. METHODOLOGY AND THEORY

The CIR Spice code files for four different logic families NOT gate are simulated using WinSpice. The input timing diagrams, output timing diagrams and VTC plots are the output result of WinSpice. Input signal with a period of 10 ns is applied to each four different NOT gates. A standard VTC plot for NOT gate is shown in Figure 1.

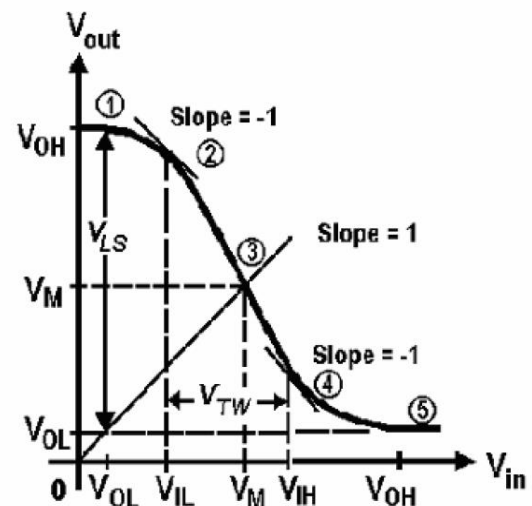


Figure 1: Standard voltage transfer characteristic (VTC) of a NOT gate

The parameters involved in VTC curve analysis are stated below:

- Output high voltage is V_{OH} . Output low voltage is V_{OL} .

- Input high voltage is V_{IH} . Input low voltage V_{IL} .
 - The midpoint voltage in the VTC where $V_O = V_I$ is V_M .
- As the input voltage is increased from 0, V_{IL} is the maximum input voltage that provides a high output voltage (logical 1 output). Furthermore, V_{IH} has the definition of being the minimum input voltage that provides a low output voltage (logical 0 output). The values V_{OH} , V_{OL} , V_{IL} and V_{IH} are referred to as the critical voltages of the voltage transfer characteristic. The midpoint voltage V_M is defined as the point on the transfer characteristic, where $V_{out} = V_{in}$ and ideally appears at the center of the transition region. V_M can be found graphically by superimposing (the unity slope) $V_{out} = V_{in}$ and finding its intersection with VTC.

In order to always distinguish between high and low voltage level, the following conditions must be satisfied:

$$V_{OH} > V_{IH} \text{ and } V_{OL} < V_{IL}$$

Furthermore, logic swing $V_{LS} = V_{OH} - V_{OL}$. Transition width $V_{TW} = V_{IH} - V_{IL}$. The transition width is the amount of voltage change that is required of the input voltage to cause a change in the output voltage from the high to the low level (or vice-versa).

Variations in the steady-state voltage levels of digital circuits (i.e. the logical 1 and the logical 0 states) are undesirable and cause logic errors if the fluctuation from the desired or specified voltage levels is too great. This variation of steady state voltage levels in digital circuits is referred to as voltage level degradation and is termed *noise*. The voltage noise margins represent a safety margin for the high and low voltage levels. Extraneous noise voltages must have magnitudes less than the voltage noise margins. The exact magnitudes of the high and low level are not important. However, the high or low magnitude of voltage must remain in the range of voltages that provide positive noise margins. High noise margin is represented by $V_{NMH} = V_{OH} - V_{IH}$, while low noise margin is represented by $V_{NML} = V_{IL} - V_{OL}$. Figure 2 shows the noise margin conditions.

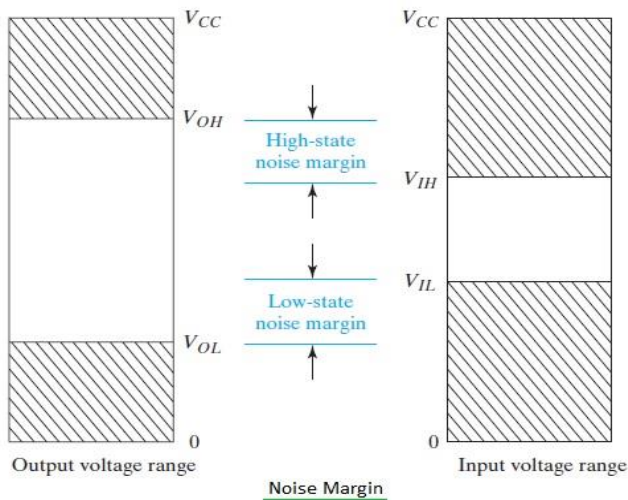


Figure 2: Noise margin conditions

- High noise sensitivity $V_{NSH} = V_{OH} - V_M$.

- Low noise sensitivity $V_{NSL} = V_M - V_{OL}$. The quantity *noise immunity* is the ability of a gate to reject noise and being defined below:

- High noise immunity $V_{NIH} = \frac{V_{NSH}}{V_{LS}}$.
- Low noise immunity $V_{NIL} = \frac{V_{NSL}}{V_{LS}}$.

Figure 3 shows the VTC for an ideal NOT gate.

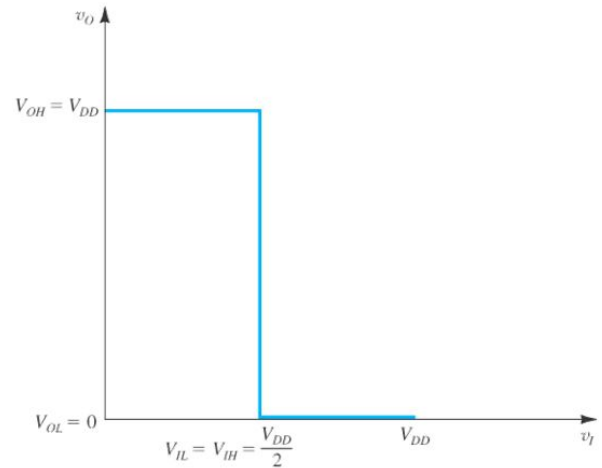


Figure 3: VTC for an ideal NOT gate

III. RESULTS AND DISCUSSIONS

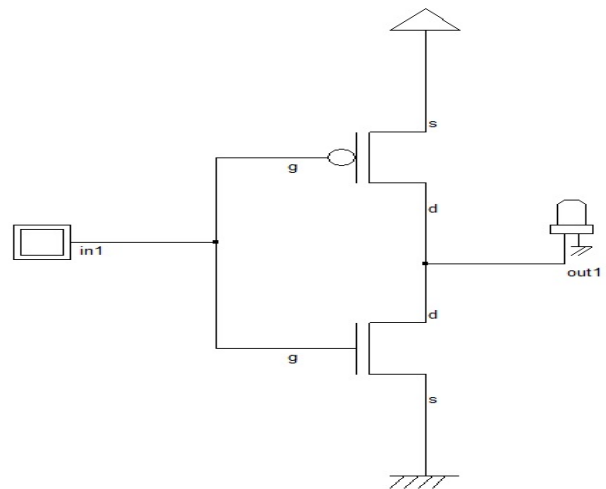


Figure 4: Nano-CMOS NOT transistor level circuit

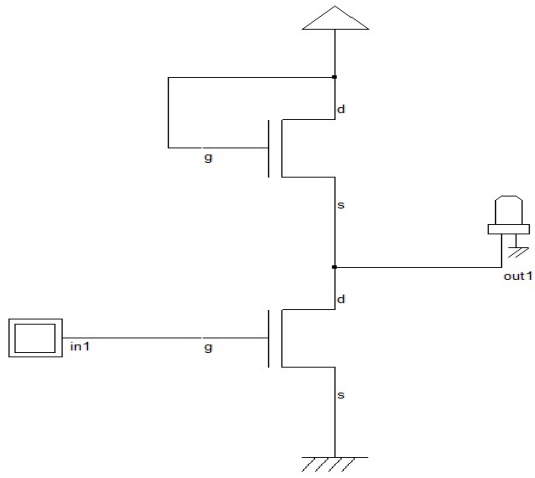


Figure 5: Nano-MOSFET loaded NOT transistor level circuit

Figure 4, Figure 5, Figure 6 and Figure 7 show the schematic circuits of all four logic families NOT gate. Their timing diagrams are shown in Figure 8(a) and 8(b), Figure 9(a) and 9(b), Figure 10(a) and 10(b) as well as Figure 11(a) and 11(b) accordingly.

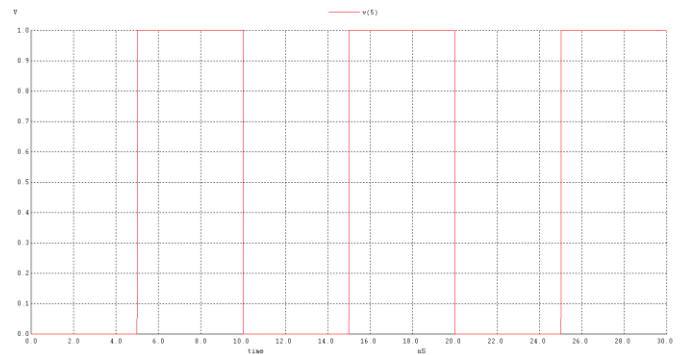


Figure 8(a): Input signal of nano-CMOS NOT circuit

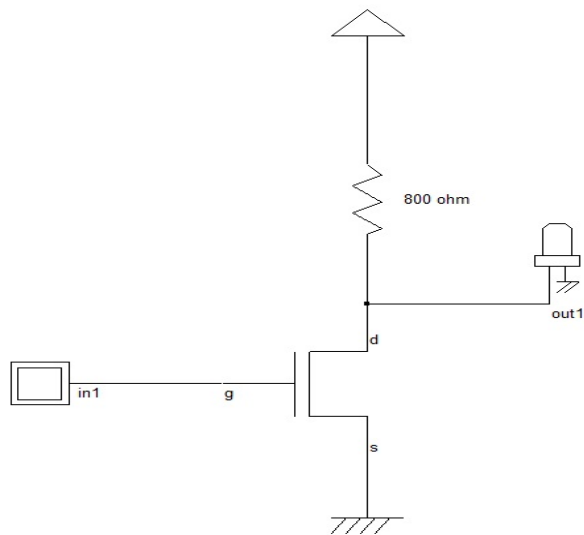


Figure 6: Resistive loaded NOT transistor level circuit

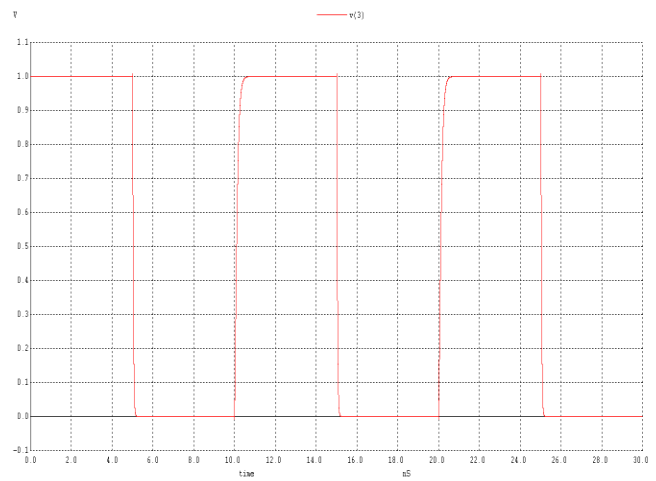


Figure 8(b): Output signal of nano-CMOS NOT circuit

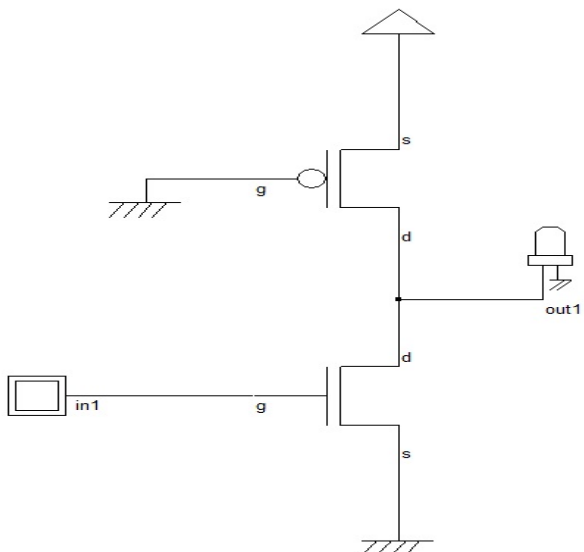


Figure 7: Pseudo nano-MOSFET NOT transistor level circuit

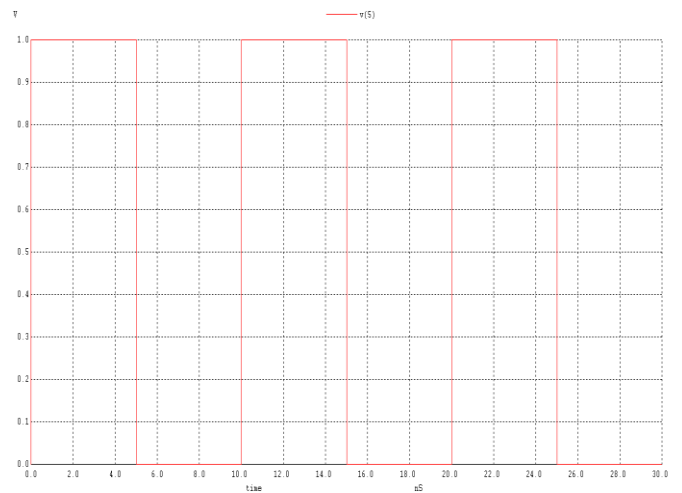


Figure 9(a): Input signal of nano-MOSFET loaded NOT circuit

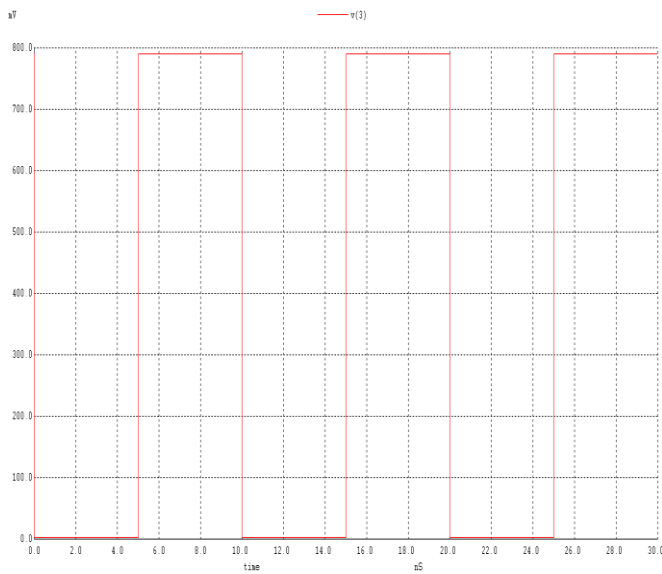


Figure 9(b): Output signal of nano-MOSFET loaded NOT circuit

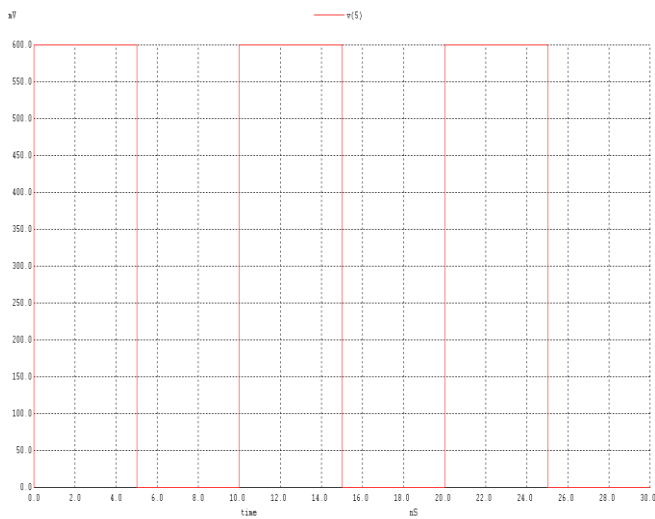


Figure 10(a): Input signal of resistive loaded NOT circuit

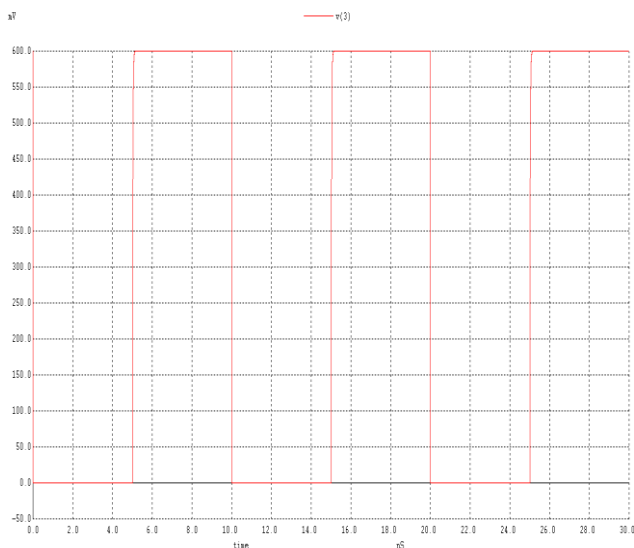


Figure 10(b): Output signal of resistive loaded NOT circuit

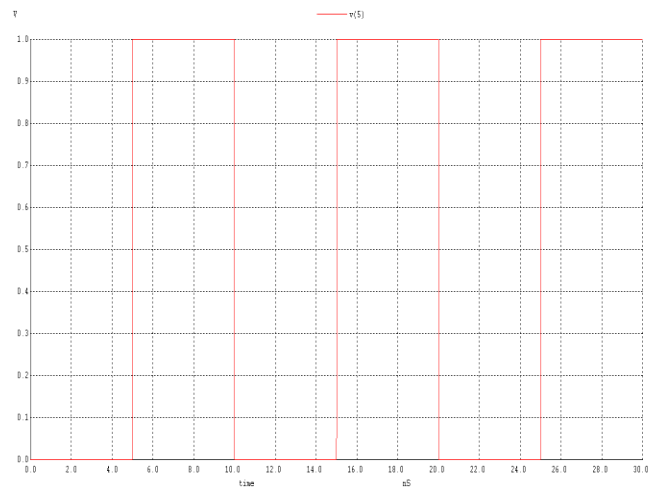


Figure 11(a): Input signal of pseudo nano-MOSFET NOT circuit

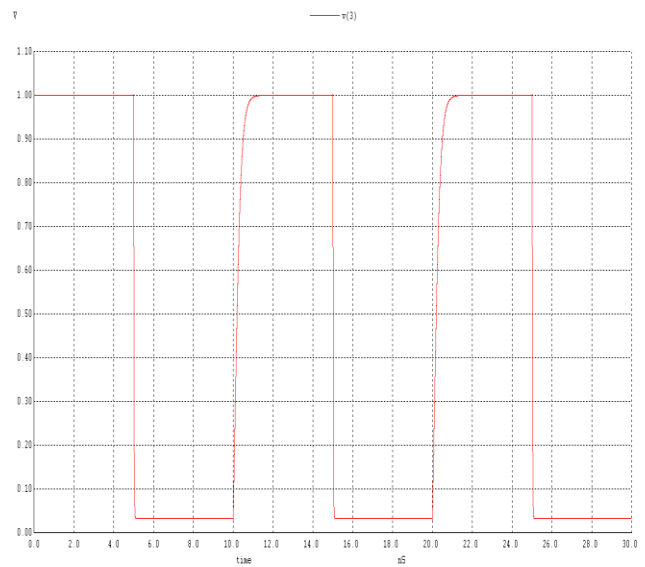


Figure 11(b): Output signal of pseudo nano-MOSFET NOT circuit

The above input and output signal timing diagrams show correct logical NOT operation for all four logic families. The period of the input signal to each NOT circuit is 10 ns. The output signal of nano-MOSFET loaded NOT circuit shows a threshold voltage loss of 0.2 V since the nano-MOSFET load acts as a pass transistor which passes a weak logic level 1 and passes a strong logic level 0. The threshold voltage loss 0.2 V corresponds to the threshold voltage of nano-MOSFET, which is 0.2 V [13, 14]. The nano-MOSFET pass transistor load is equivalent to 800 Ω load resistance. This 800 Ω resistance is calculated from the nano-MOSFET current-voltage (I-V) curve in the linear portion, where digital operation occurred as shown in Figure 12. By this way, resistive loaded 800 Ω nano-MOSFET NOT circuit is formed as shown in Figure 6.

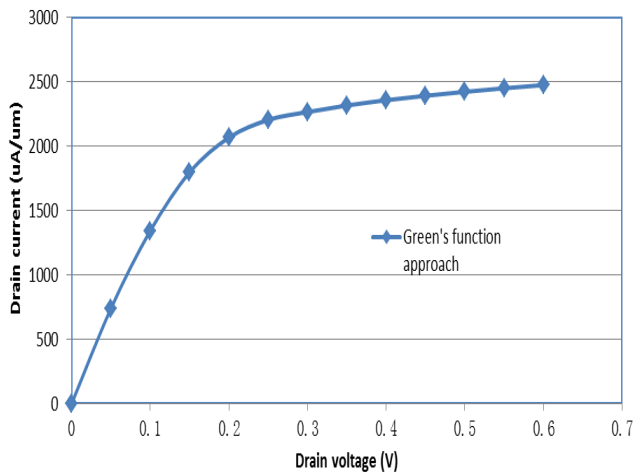


Figure 12: I-V curve of nano-MOSFET. Linear portion of this curve is used to calculate load resistance.

Figure 13, Figure 14, Figure 15 and Figure 16 show the VTC plots of all four logic families NOT circuit.

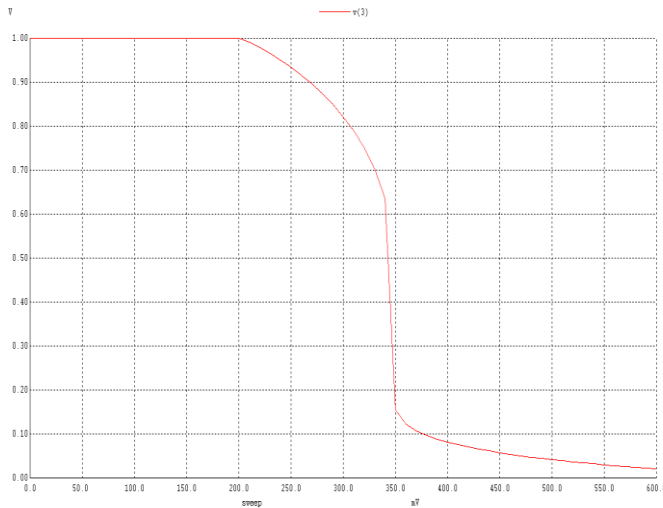


Figure 13: Simulated VTC curve of nano-CMOS NOT circuit

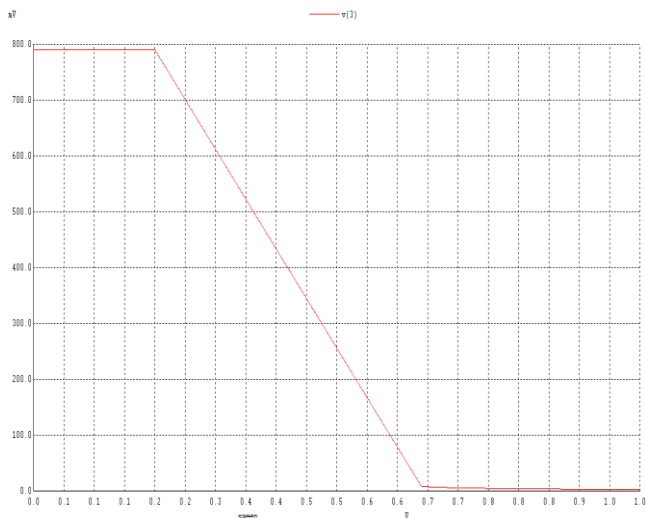


Figure 14: Simulated VTC curve of nano-MOSFET loaded NOT circuit

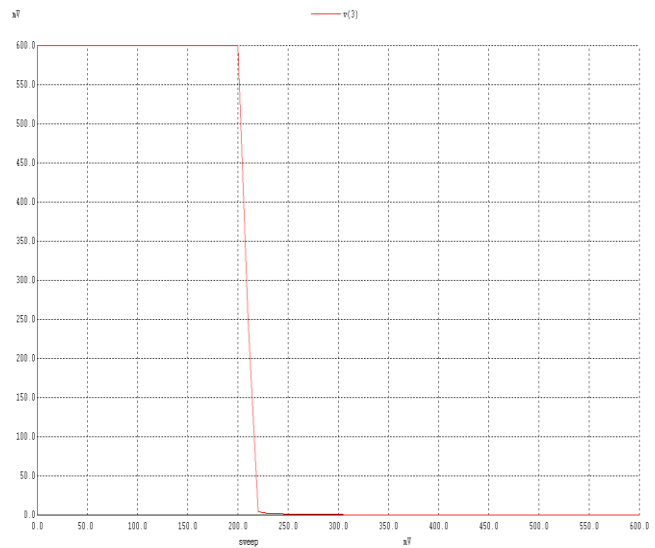


Figure 15: Simulated VTC curve of resistive loaded NOT circuit

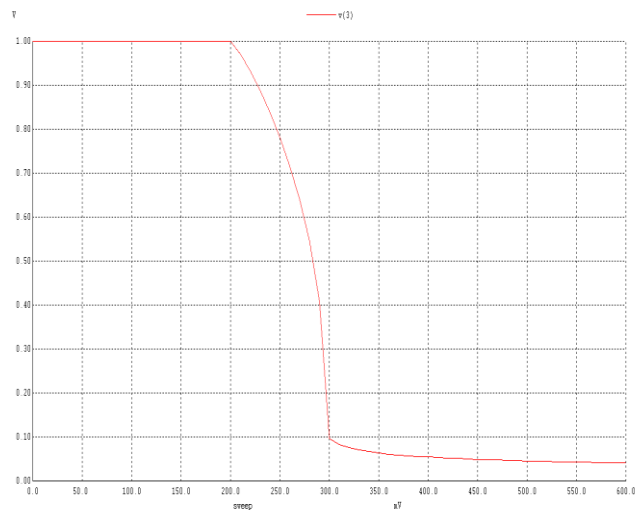


Figure 16: Simulated VTC curve of pseudo nano-MOSFET NOT circuit

Table 1, Table 2, Table 3 and Table 4 are the parameters calculated from the VTC plots using the expressions explained in the previous section. From these tables, the analysis indicates that the condition $V_{OH} > V_{IH}$, $V_{OL} < V_{IL}$ and noise margins are met. Therefore, all four logic NOT gates designs formed by p-type and n-type nano-MOSFETs with channel length $L=10$ nm and width $W=125$ nm or 250 nm can work properly. In nano-CMOS NOT circuit, n-type nano-MOSFET has $W=125$ nm and p-type nano-MOSFET has $W=250$ nm to counter-balance the difference in electron and hole mobility. In nano-MOSFET loaded NOT circuit, the n-type nano-MOSFET load has $W=125$ nm and the bottom n-type nano-MOSFET has $W=250$ nm. This condition is needed to meet

$$\left(\frac{W}{L}\right)_n \geq 2\left(\frac{W}{L}\right)_{Load}$$

in order to reduce V_{OL} .

Table 1: VTC parameters for nano-CMOS NOT circuit

Nano-CMOS NOT Circuit	
V _{OH}	1.00 V
V _{OL}	0.02 V
V _{IH}	0.40 V
V _{IL}	0.20 V
V _M	0.35 V
V _{LS}	0.98 V
V _{TW}	0.20 V
V _{NMH}	0.60 V
V _{NML}	0.18 V
V _{NSH}	0.65 V
V _{NSL}	0.33 V
V _{NIH}	0.66
V _{NIL}	0.37

Table 2: VTC parameters for nano-MOSFET loaded NOT circuit

Nano-MOSFET loaded NOT Circuit	
V _{OH}	0.80 V
V _{OL}	0.00 V
V _{IH}	0.66 V
V _{IL}	0.20 V
V _M	0.42 V
V _{LS}	0.80 V
V _{TW}	0.42 V
V _{NMH}	0.14 V
V _{NML}	0.20 V
V _{NSH}	0.38 V
V _{NSL}	0.42 V
V _{NIH}	0.48
V _{NIL}	0.52

Table 3: VTC parameters for resistive loaded NOT circuit

Resistive loaded 800Ω NOT Circuit	
V _{OH}	0.60 V
V _{OL}	0.00 V
V _{IH}	0.22 V
V _{IL}	0.20 V
V _M	0.21 V
V _{LS}	0.60 V
V _{TW}	0.02 V
V _{NMH}	0.38 V
V _{NML}	0.20 V
V _{NSH}	0.39 V
V _{NSL}	0.21 V
V _{NIH}	0.65
V _{NIL}	0.35

Table 4: VTC parameters for pseudo nano-MOSFET NOT circuit

Pseudo nano-MOSFET NOT Circuit	
V _{OH}	1.00 V
V _{OL}	0.05 V
V _{IH}	0.30 V
V _{IL}	0.20 V
V _M	0.28 V
V _{LS}	0.95 V
V _{TW}	0.10 V
V _{NMH}	0.70 V
V _{NML}	0.15 V
V _{NSH}	0.72 V
V _{NSL}	0.23 V
V _{NIH}	0.76
V _{NIL}	0.24

In pseudo nano-MOSFET NOT circuit, p-type nano-MOSFET has W = 125 nm and n-type nano-MOSFET has W = 250 nm. This condition is needed to meet the same criteria in the above expression in order to reduce V_{OL}. Meanwhile, in the resistive loaded 800 Ω NOT circuit, 800 Ω resistance is the load and n-type nano-MOSFET has W = 250 nm [15].

The effects of down scaling of MOSFET into nanometer regime, which will be discussed now include drain current, intrinsic delay and dynamic power. If the scaling factor is s, Table 5 lists the quantities of MOSFET involved in the down scaling.

Table 5: Quantities of MOSFET involved in down scaling

Quantity	Before Scaling	After Scaling
Channel Length	L	L'=L*s
Channel Width	W	W'=W*s
Gate Oxide Thickness	T _{OX}	T' _{OX} =T _{OX} *s
Power Supply	V _{DD}	V' _{DD} =V _{DD} *s
Threshold Voltage	V _{TH}	V' _{TH} =V _{TH} *s

For scaling purpose, the alpha-power model of drain current is very useful:

$$I_{DS} = KWL^{-0.5}T_{OX}^{-0.8}(V_{GS} - V_{TH})^{1.25}$$

where K is the process transconductance. If L, T_{OX} and V are all scaled by the scaling factor s, current should remain constant per micron of width (approximately 2500 μA/μm, refer to Figure 12). Since capacitance is

$$C = \frac{\epsilon WL}{T_{OX}}$$

the intrinsic delay is given by:

$$\Delta t' = \frac{CV}{I} = s\Delta t$$

since C, V and I all were scaled down by the scaling factor s. Hence, logic gate formed by down scaled MOSFET has smaller delay and performed faster. To investigate the dynamic power during down scaled, refer to Table 6. The drain/source capacitance of nano-MOSFET is 1.184×10^{-16} F.

Table 6: Dynamic powers for four different NOT logic

	nano-CMOS NOT	nano-MOSFET loaded NOT	Pseudo nano-MOSFET NOT	Resistive loaded NOT
Dynamic Power (Watts)	2.36E-08	2.36E-08	2.36E-08	7.10E-09
Voltage Supply (Volts)	1	1	1	0.6
Frequency of switching (Hertz)	1.00E+08	1.00E+08	1.00E+08	1.00E+08

The equation used to obtain dynamic power is:

$$P(\text{dyn}) = C f V_{DD}^2.$$

where C is the capacitance at output node, f is the frequency of switching and V_{DD} is the voltage supply. Normally, in conventional bulk micrometer MOSFET logic, the dynamic power is about μW . Therefore, from Table 6, reduction in dynamic power is observed during down scaling.

IV. CONCLUSION

Logical NOT gate operation can be implemented by using nano-MOSFETs with four different logic families. Conventional bulk MOSFETs can be replaced by nano-MOSFETs to implement NOT transistor level circuits. In this paper, this development in semiconductor industry has been shown by a simulation study using WinSpice and observing the input timing diagrams, output timing diagrams and VTC plots. Correct logical NOT operations are observed from these simulation output. During the down scaling process, a faster logic gate is possible when the current per micron width remain constant, dynamic power is reduced and intrinsic delay becomes slower.

REFERENCES

- [1] Reza Hosseini and Neda Teimourzadeh, "Simulation study of circuit performance of GAA silicon nanowire transistor and DG MOSFET," *Physical Review & Research International*, 3(4): 568-576, 2013.
- [2] P. A. Gowri Sankar and K. Udhayakumar, "MOSFET-like CNFET based logic gate library for low-power application: a comparative study," *Journal of Semiconductors*, Vol. 35, No. 7, 2014.
- [3] Ulrich Wulf, Marcus Krahlisch and Hans Richter, "Scaling properties of ballistic nano-transistors," *Nanoscale Research Letters*, 6:365, 2011.
- [4] Marc Baldo, "Introduction to nanoelectronics," *MIT OpenCourseWare Publication*, May 2011.
- [5] K. Navi, M. Rashtian, A. Khatir, P. Keshavarzian and O. Hashemipour, "High speed capacitor-inverter based carbon nanotube full adder," *Nanoscale Research Letters*, 5:859-86, 2010.
- [6] Michael Loong Peng Tan, Georgios Lentaris and Gehan AJ Amaratunga, "Device and circuit-level performance of carbon nanotube field-effect transistor with benchmarking against a nano-MOSFET," *Nanoscale Research Letters*, 7:467, 2012.
- [7] Huei Chaeng Chin, Cheng Siong Lim, Weng Soon Wong and Michael Loong Peng Tan, "Enhanced device and circuit-level performance benchmarking of graphene nanoribbon field-effect transistor against a nano-MOSFET with interconnects," *Journal of Nanomaterials*, Vol. 2014, Article ID 879813.
- [8] Rohini Gupta, Bogdan Tutuianu and Lawrence T. Pileggi, "The Elmore delay as a bound for RC trees with generalized input signals," *IEEE Transactions on Computer-Aided Design of Integrated Circuits and Systems*, Vol. 16, No. 1, 95-104, 1997.
- [9] Yiming Li and Chih-Hong Hwang, "High-frequency characteristic fluctuations of nano-MOSFET circuit induced by random dopants," *IEEE Transactions on Microwave Theory and Techniques*, Vol. 56, No. 12, 2726-2733, 2008.
- [10] Ming-Hung Han, Yiming Li and Chih-Hong Hwang, "The impact of high-frequency characteristics induced by intrinsic parameter fluctuations in nano-MOSFET device and circuit," *Microelectronics Reliability*, 50, 657-661, 2010.
- [11] A. A. A. Nasser, Moustafa H. Aly, Roshdy A. AbdelRassoul, Ahmed Khourshed, "Performance of near-ballistic limit carbon nano-transistor (CNT) circuits," *ICCTA*, 175-182, 2011.
- [12] Hesham F. A. Hamed, Savas Kaya and Janusz A. Starzyk, "Use of nano-scale double-gate MOSFETs in low-power tunable current mode analog circuits," *Analog Integr Circ Sig Process*, doi 10.1007/s10470-008-9134-4, 2008.
- [13] Ooi Chek Yee and Lim Soo King, "Simulation study on the electrical performance of equilibrium thin-body double-gate nano-MOSFET," *Jurnal Teknologi*, Vol. 76, 87-95, 2015.
- [14] Ooi Chek Yee and Lim Soo King, "Simulation study of 2D electron density in primed and unprimed subband thin-body double-gate nano-MOSFET of three different thicknesses and two temperature states," *International Journal of Nanoelectronics and Materials*, Vol. 9, 67-84, 2016.
- [15] Sanjeet Kumar Sinha and Saurabh Chaudhury, "Simulation and analysis of quantum capacitance in single-gate MOSFET, double-gate MOSFET and CNFET devices for nanometer regime," *IEEE* 978-1-4673-4700-6, 2012.